TITLE PAGE

Journal:

Biomedical Signal Processing and Control

Title of paper:

Uterine contractile efficiency indexes for labor prediction: a bivariate approach from multichannel electrohysterographic records.

Authors and addresses

J. Mas-Cabo[1], Y. Ye-Lin[1], J. Garcia-Casado[1], J. Alberola-Rubio[2], A. Perales[2], G. Prats-Boluda[1]

[1]Centro de Investigación e Innovación en Bioingeniería, Universitat Politècnica de València, Camino de Vera s/n Ed.7F, 46022 Valencia, Spain:jmas@ci2b.upv.es, gprats@ci2b.upv.es, jgarciac@ci2b.upv.es, yiye@ci2b.upv.es

[2]Servicio de Obstetricia, H.U. P. La Fe, Valencia, Spainpalberola.rubio@gmail.com; Perales_alf@gva.es

Contact information for corresponding author:

Name: Gema Prats Boluda

Phone Nº: 3496-3877007 ext. 76067

Email: gprats@ci2b.upv.es

ABSTRACT

Labor prediction is one of the most challenging goals in obstetrics, mainly due to the poor understanding of the factors responsible for the onset of labor. The electrohysterogram (EHG) is the recording of the myoelectrical activity of myometrial cells and has been shown to provide relevant information on the electrophysiological state of the uterus. This information could be used to obtain more accurate labor predictions than those of the currently used techniques, such as the Bishop score, tocography or biochemical markers. Indeed, a number of efforts have already been made to predict labor by this method, separately characterizing the intensity, the coupling degree of the EHG signals and myometrial cell excitability, these being the cornerstones on which contraction efficiency is built. Although EHG characterization can distinguish between different obstetric situations, the reported results have not been shown to provide a practical tool for the clinical detection of true labor. The aim of this work was thus to define and calculate indexes from multichannel EHG recordings related to all the phenomena involved in the efficiency of uterine myoelectrical activity (intensity, excitability and synchronization) and to combine them to form global efficiency indexes (GEI) able to predict delivery in less than 7/14 days. Four EHG synchronization indexes were assessed: linear correlation, the imaginary part of the coherence, phase synchronization and permutation cross mutual information. The results show that even though the synchronization and excitability efficiency indexes can detect increasing trends as labor approaches, they cannot predict labor in less than 7/14 days. However, intensity seems to be the main factor that contributes to myometrial efficiency and is able to predict labor in less than 7/14 days. All the GEIs present increasing monotonic trends as pregnancy advances and are able to identify ($p < 0.05$) patients who will deliver in less than 7/14 days better than single channel and single phenomenon parameters. The GEI based on the permutation cross mutual information shows especially promising results. A simplified EHG recording protocol is proposed here for clinical practice, capable of predicting

deliveries in less than 7/14 days, consisting of 4 electrodes vertically aligned with the median line of the uterus.

Keywords: Electrohysterogram, synchronization, nonlinear analysis, efficiency indexes.

1. INTRODUCTION

Electrohysterography (EHG) or uterine electromyography has arisen as a non-invasive monitoring technique for assessing uterine dynamics and predicting the onset of labor. Compared with the currently used prediction techniques, based on monitoring uterine dynamics, such as tocography, the Bishop Score or biochemical markers, the use of EHG in clinical practice would lead to more accurate diagnosis and prediction of true labor [1], thus avoiding unnecessary hospitalizations and reducing healthcare costs. This is especially relevant in threatened preterm patients, since preterm birth is one of the leading causes of neonatal morbidity in the developed countries and often involves expensive interventions [2,3].

Predicting labor within 7 days is the most commonly studied time horizon in the literature [4] as it has clinical relevance; tocolysis has been shown to reduce the risk of delivery within 48 hours and 7 days [5] and is usually prescribed to allow administration of glucocorticoids and reduce the risk of prematurity complications. However, there are other studies on 14-day labor prediction which provide advantageous information for pregnancy and labor management [6,7]. The obstetrical indicators traditionally employed for labor prediction, such as cervical length, Bishop Score, or number of contractions/10 minutes, do not provide results reliable enough for predicting imminent labor [4,8]. Although cervical length is one of the most widely used labor prediction indicators in clinics [7,9], several studies report that this criterion has proved to be insufficient or inaccurate in predicting labor [9,10]. Due to its low positive predictive values and sensitivities, routine cervical length assessment is not recommended in women at low risk of preterm labor [9]. Conversely, electrohysterographic techniques have arisen as potential labor prediction tools, yielding better results than the traditional obstetrical parameters [10,11].

The EHG registers the electrical activity associated with the contraction of the myometrial cells and can be recorded by placing electrodes on the abdominal surface [12]. Several studies found that EHG features change throughout pregnancy [13]. Uterine electrical activity is weak and uncoordinated in the early gestational ages, but becomes more coordinated and intense as pregnancy progresses [12,13]. The first studies carried out on women and animal subjects in the 90s revealed that EHG could provide valuable information on the progression of pregnancy and the onset of labor [13,14].

The EHG signal is made up of the register of the basal tone (associated with the resting state of the uterus) and the EHG-bursts (which represent the electrical activity associated with uterine contractions). Most authors in this field focus on the [0.1 - 4] Hz range, since it is considered that EHG spectral content is mainly distributed in this range [15]. EHG features related to the excitability phenomenon have been studied, usually extracting parameters from the power density spectrum of the EHG-bursts, such as peak, mean or median frequencies [6,15,16].

Regarding EHG-burst synchronization, various indexes, such as linear and non-linear correlation, have been proposed to quantify the evolution of the coupling between different EHG recording channels to obtain information on labor onset [17], the imaginary part of the coherence [18] and others based on phase synchronization [19]. Although they all have shown higher synchronization values for the labor groups, there is still no consensus on the most appropriate method of evaluating EHG signals synchronization, since each synchronization index evaluates different aspects. Both the linear and non-linear correlation indexes evaluate signal coupling in the temporal domain, while the coherence-based indexes operate in the EHG spectrum, and still others estimate the degree of coupling by the phase differences. Synchronization indexes which evaluate coupling from the mutual information shared between different time series, especially the permutation cross mutual information (PCMI), has shown promising results in electroencephalographic applications [20].

However, as far as we know, there are no studies which evaluate all the different factors involved in the efficiency of myoelectrical activity through the analysis of multichannel EHG registers, nor has a global-efficiency index yet been defined that combines the uterine activity intensity, cellular excitability and synchronization. Such an analysis would provide valuable information on the mechanisms that initiate labor.

Some authors have already employed spectral, temporal and EHG synchronization parameters to predict labor and non-labor situations or classify patients into term or preterm labor [21–23]. However, even though some have reported high accuracy values, these results are usually limited by different factors, such as a strong dependence on electrode configuration or controversial values obtained from different databases [24,25], so that the reported results have not been shown to provide a practical tool for the clinical detection of true labor. As there is therefore still a need for robust global myoelectrical activity indexes which can predict labor in common clinical conditions, the aim of this work was to obtain robust myoelectrical uterine activity efficiency indexes to identify the expectant mothers who will deliver in less than 7/14 days. For this, the evolution of different single-phenomenon efficiency indexes (which include information on intensity, excitability and synchronization of the uterine contractile events) was first studied and then combined to define uterine activity global efficiency indexes. A reduced electrode set was also evaluated to facilitate the use of the EHG technique in clinical practice and avoid the entangled and complex acquisition protocols and systems associated with a large number of channel registers.

2. MATERIALS & METHODS

A. DATABASE

The "Icelandic 16-electrode database"[26] was chosen for this work as it contains a collection of multichannel EHG pregnancy and labor recordings to facilitate the study of the evolution of uterine contraction efficiency indexes in different stages of labor.

This database includes 122 EHG registers from 45 pregnant women: 112 during pregnancy (third trimester) and the rest during labor (patients who delivered within 24 h). The subjects had normal singleton pregnancies and unknown preterm labor risk factors.

As the aim was to obtain information on the labor horizon from the myoelectrical activity during pregnancy, the recordings were divided into different groups by time-to-delivery (TTD). The records were classified as follows: patients recorded during labor, those who delivered between 1 and 7 days after the recording session, those who gave birth between 7 and 14 days after the recording session, those who delivered between 14 to 30 days, and those who gave birth after more than 30 days (See Figure 1). The recordings were also used to analyze the indexes' ability to predict deliveries in less than 7 days (Grouping the labor and TTD 1-7 day patients) and 14 days (Grouping the labor, TTD 1-7 day and TTD 7-14 day patients) after the recording session.

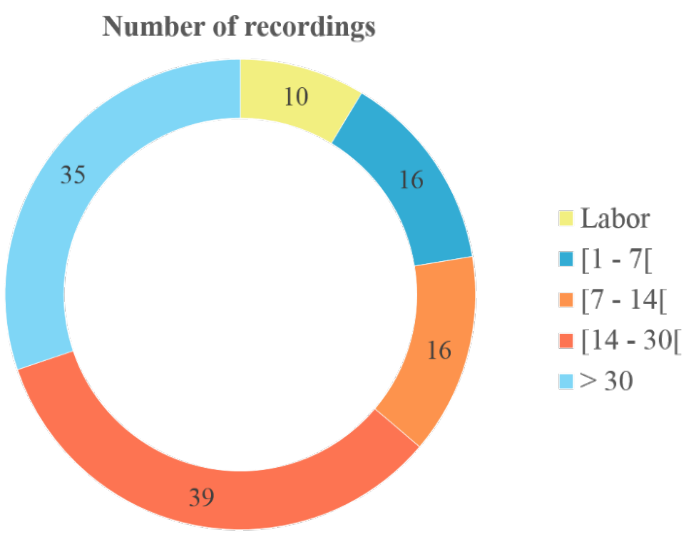

Figure 1: Distribution of registers according to time-to-delivery (in days).

B. DATA ANALYSIS

The database provides monopolar raw records of EHG signals from a grid of 4x4 electrodes. The EHG monopolar signals were resampled at 20 Hz and digitally filtered in the range 0.1 to 4 Hz using a 5th order Butterworth bandpass digital filter, since EHG spectral content is mainly distributed in this range [15]. After monopolar signal pre-processing 12 vertical bipolar signals were obtained, as seen in Figure 2. All the analyses in this work were performed on bipolar signals, since they have been reported to have a better signal to noise ratio and immunity against common mode interference than monopolar recordings [27–29]. Only the signal segments of uterine contractions were analyzed. EHG-bursts were then manually segmented by specialists under the supervision of obstetricians. They were identified by the presence of significant amplitude and frequency changes with respect to the basal tone, with durations greater than 40 s and absence of evident motion artifacts [30]. We discarded 8/122 recordings because of persistent and significant motion artifacts or respiratory interference throughout the recording.

As already mentioned, the evolution of the different phenomena involved in myoelectrical activity efficiency were analyzed separately and combined into global efficiency indexes. The capacity of all the indexes to accurately predict labor in more than 7/14 days was also analyzed. Single-phenomenon efficiency indexes were defined to estimate the intensity, excitability and synchronization of uterine activity.

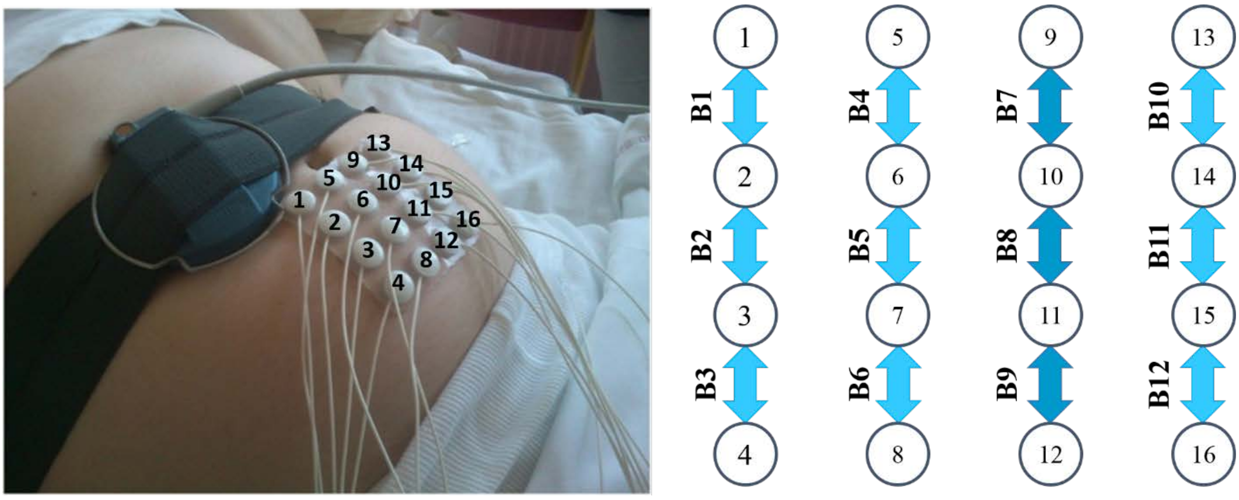

Figure 2: Electrode numbering scheme of the Icelandic data-base and method of calculating bipolar signals (adapted from the original work "Icelandic 16-electrode database" [26]*).*

B.1 *Single-phenomenon Efficiency Indexes*

Labor is known to be preceded by two physiological phenomena: increased connectivity of the myometrial cells and increased excitability [7,12]. The former is related to an increase in the number of GAP junctions, which allow intercellular communication and so better propagation of action potentials [5,12]. The higher the uterine cell connectivity involved in the contraction, the higher the contraction intensity (EHG signal amplitude). As the cells are more coordinated, the synchronization values between signals recorded in different channels are expected to be higher as labor approaches [31]. On the other hand, the increased cell excitability is related to the expression of more oxytocin receptors by myometrial cells as labor approaches [13,32] and produces the higher frequency components present in EHG signals [33,34]. EHG parameters related to the excitability, intensity and synchronization phenomena computed from single and multi-channel EHG recordings are thus expected to show higher values in women closer to labor.

B.1.1 *Single channel Efficiency Indexes*

In many of the studies carried out previously, the information from each bipolar record is used separately [35–37]. As already mentioned, amplitude and spectral parameters are related to the intensity and excitability of the myometrial cells, respectively. To assess the ability of each EHG channel to predict imminent delivery, the average rectified value (ARV [38]) of the EHG-bursts and the dominant frequency (DF [34,39]) were computed as follows:

$$SC\_IEI = ARV_a = \frac{1}{N}\sum_{i=1}^{N}|X_a(i)| \quad (1)$$

Where *N* is the length of the data vector $X_a(i)$ in samples.

$$SC\_EEI = DF_a = \mathrm{W}_a(\max(peaks(PSD_{0.2Hz}^{1Hz}))) \quad (2)$$

Where W_a consists in a vector which represent each frequency value of the PSD computed in the range 0.2 to 1 Hz.

B.1.2 *Multi-channel Intensity Efficiency Index (IEI)*

In order to quantify the EHG-burst amplitude recorded by the different surface electrodes, a multichannel intensity efficiency index (MC_IEI) is defined for each pair of bipolar records as:

$$MC\_IEI_{ab} = \sqrt{ARV_a \cdot ARV_b} \quad (3)$$

Where ARV_a and ARV_b are the average rectified value of temporal series $a(t)$ and $b(t)$, respectively [38].

B.1.3 *Multi-channel Excitability Efficiency Index (EEI)*

As cell excitability is directly related to the spectral content of the recorded signals [40], we defined a multichannel excitability efficiency index (MC_EEI) which reflects the spectral content of two different simultaneously recorded EHG signals as follows:

$$MC\_EEI_{ab} = \sqrt{DF_a \cdot DF_b} \quad (4)$$

Where DF_a and DF_b are the dominant frequencies of temporal series $a(t)$ and $b(t)$, respectively.

The efficiency of uterine contractility depends on the excitability and the degree of coupling of electrical activity, so that highly efficient EHG-bursts can be expected to present higher IEI and EEI values.

B.1.4 *Synchronization Efficiency Indexes (Multi-channel)*

Cross correlation (COR)

Cross correlation evaluates the linear correlation between two time series $a(t)$ and $b(t)$ with lag T[41] and is defined as:

$$COR_{ab}(T) = \frac{cov_{ab}(t, t+T)}{\sqrt{var_a(t) * var_b(t+T)}} \quad (5)$$

Where var, represents the variance of each series, and cov is the covariance between the two time series. The *COR* values are restricted to the [-1, 1] range, where values close to "1" mean high linear synchronization and negative COR means weak synchronization between the two time series.

Imaginary part of coherence (iCOH)

Coherence provides the linear correlation between two time series $a(t)$ and $b(t)$in the frequency domain [41] and is defined as the cross spectral density function (C_{ab}) divided by the individual auto spectral density functions (C_{aa} and C_{bb}). Some authors found that the use of the imaginary part of the coherence function could reduce the effect of the volume conductor [42], and is defined as:

$$NC_{ab}(f) = \frac{|ImC_{ab}(f)|}{\sqrt{|C_{aa}(f)| * |C_{bb}(f)|}} \quad (6)$$

Where ImC_{ab} is the imaginary part of the cross spectral density function.The result is a function with values between "0" and "1", "1" being the maximum degree of synchronization. In order to assess

EHG-burst synchronization, the $iCOH_{ab}$ index is defined across the frequency band [0.34 – 1] Hz as [43]:

$$iCOH_{ab} = \frac{1}{N}\sum_{f=0.34}^{1} NC_{ab}(f) \quad (7)$$

Where N is the total number of elements in the summand and the $iCOH_{ab}$ index ranges from 0 to 1.

Phase synchronization (PLV)

The phase synchronization hypothesis states that dynamic systems may have their phases synchronized even if their amplitudes are not correlated. Of the different phase synchrony estimations, in this study we focused on the phase locking value (PLV) as it has shown good performance in measuring the coupling degree of other phase synchronization indexes [20,44]. The PLV index is defined as:

$$PLV_{ab} = \frac{1}{N}\left|\sum_{t=1}^{N} e^{i\Delta\phi_{ab}(t)}\right| \quad (8)$$

Where $\Delta\phi_{ab}(t)$ is the difference between the instantaneous phase of the two time series, $\phi_a(t)$ and $\phi_b(t)$. *PLV* values range between “0” and “1”, “1” being the maximum synchronization degree between two dynamic systems.

Normalized permutation cross mutual information (NPCMI)

This synchronization index, based on the calculation of the probability distribution of the order patterns [20], performs an order pattern analysis. From two time series $a(t)$ and $b(t)$ two respective embedding vectors can be obtained $a_i(t) = [a(i), a(i+T), \ldots, a(i + (m + 1)T)]$ and $b_i(t) = [b(i), b(i+T), \ldots, b(i + (m + 1)T)]$, where m is the embedding dimension and T the time lag. The possible m! order patterns are obtained by sorting the embedding vectors in ascending order, these patterns also receive the name of permutations [20]. Then the probability of each permutation $p_a(k_a)$ and $p_b(k_b)$ are calculated as:

$$p_a(k_a) = \frac{C_a(k_a)}{N-(m-1)T} \ (9) \ ; \qquad p_b(k_b) = \frac{C_b(k_b)}{N-(m-1)T} \ (10)$$

Where $C_a(k_a)$ $(k_a = 1, 2, \ldots, m!)$ and $C_b(k_b)$ $(k_b = 1, 2, \ldots, m!)$ are the number of each order pattern. The permutation entropy PE_a and PE_b, based on Shannon's information theory, can be expressed as [20]:

$$PE_a = -\sum_{k_a=1}^{m!} p_a(k_a)\ln\big(p_a(k_a)\big)\ (11)\ ;\qquad PE_b = -\sum_{k_b=1}^{m!} p_b(k_b)\ln\big(p_b(k_b)\big)\ (12)$$

And so the joint permutation entropy of the time series $a(t)$ and $b(t)$ is [20]:

$$PE_{ab} = -\sum_{k_a=1}^{m!}\sum_{k_b=1}^{m!} p_{ab}(k_a, k_b)\ln\big(p_{ab}(k_a, k_b)\big)\ (13)$$

Where p_{ab} is the joint probability of permutation embedding vectors a_i and b_i. Now the PCMI of the two time series can be expressed as follows:

$$PCMI_{ab} = PE_a + PE_b - PE_{ab}\ (14)$$

And finally the PCMI can be normalized as follows [45]:

$$NPCMI_{ab} = \frac{PCMI_{ab}}{\min\{PE_a, PE_b\}}\ (15)$$

NPCMI finally ranges between values of [0, 1]; values close to "1" again signify a strong synchronization relationship between the two time series.

B.2 *Global Efficiency indexes (GEI)*

Although the above described indexes provide some information on myoelectrical activity efficiency, none of them contains information on all the phenomena involved in the efficiency of myoelectrical activity. We therefore developed the global efficiency indexes (GEIs), which combine the synchronization indexes with the intensity and excitability indexes as follows (multichannel):

$$GEI1_{ab} = MC\_IEI_{ab} \cdot MC\_EEI_{ab} \cdot COR_{ab}\ (16)$$

$$GEI2_{ab} = MC\_IEI_{ab} \cdot MC\_EEI_{ab} \cdot iCOH_{ab}\ (17)$$

$$GEI3_{ab} = MC\_IEI_{ab} \cdot MC\_EEI_{ab} \cdot PLV_{ab}\ (18)$$

$$GEI4_{ab} = MC\_IEI_{ab} \cdot MC\_EEI_{ab} \cdot NPCMI_{ab}\ (19)$$

B.3 *Mean efficiency indexes (MEI)*

For every EHG-burst, each single-phenomenon and global efficiency index was calculated for every pair of bipolar recordings, except the corresponding bipolar recording with itself (single-channel approach), obtaining a 12x12 myoelectrical activity efficiency matrix (C_{ij} where sub-indexes *i=1…12* and *j=1…12* represent a bipolar recording) with null values in the diagonal. For each recording session, "N_{12x12}" matrices were obtained for "N" embedded EHG-bursts.

All this information was intended to be summarized into a single index of contractile efficiency for which these "N" matrices were averaged, obtaining a single 12x12 average efficiency matrix ($\overline{C_{ij}}$) of the EHG-bursts present in each record (See diagram shown in Figure 3A). Finally the average value of the upper triangular part of the average efficiency matrix ($\overline{C_{ij}}$) was computed so as to obtain a single value per efficiency index for each recording session (losing the spatial information). These mean efficiency indicators (MEI) were calculated for every efficiency index in each recording session. The evolution of MEI values throughout pregnancy and their discriminating capacity for predicting labor in less than 7/14 day was then studied.

$$MEI = \frac{1}{\sum_{k=1}^{\frac{M^2-M}{2}} k} * \left[\sum_{i=1}^{M-1} \sum_{j=i+1}^{M} \overline{C_{ij}} \right] \quad (20)$$

Where ($\overline{C_{ij}}$) represents the average efficiency matrix for every efficiency index and M represents the total number of bipolar recordings (M = 12).

To evaluate the efficiency indexes ability to predict labor in less than 7/14 days and more than 7/14 days, respectively, the MEI values were compared (TTD<7d vs. TTD>7d and TTD<14d vs. TTD>14d) by the Wilcoxon ranked test ($\alpha = 0.05$).

B.4 *Analysis of a reduced recording set*

The multichannel approach described in the previous sections uses 12 bipolar EHG channels obtained from a 4x4 grid of electrodes. However, so many electrodes and such a big recording area may not be suitable for clinical practice, in which access to the patient and leaving room for other monitoring devices are priorities. To propose a reduced EHG recording set that uses the information from fewer electrodes and a smaller recording area, a search was made for the pairs of recording channels best able to detect time to delivery. This was performed only with the GEI that yielded the lowest p-value in the previous MEI analysis.

The statistical differences of each pair of bipolar recordings of the average efficiency matrix ($\overline{C_{ij}}$, without losing the spatial information) were compared between TTD<7d vs. TTD>7d and TTD<14d vs. TTD>14d by the Wilcoxon ranked test (α=0.05). The number of elements of the average efficiency matrix ($\overline{C_{ij}}$, j=1…12 and $j \neq i$) that presented significant differences for discriminating labor in less than 7/14 days was noted for each bipolar recording channel (row or column) i, the maximum number being 11 (See Figure 3B).

Based on the results of this procedure, a simplified EHG recording protocol was proposed with a reduced number of bipolar records for distinguishing labor in less than 7/14 days. The discrimination capacity of this reduced set of recording channels was also tested.

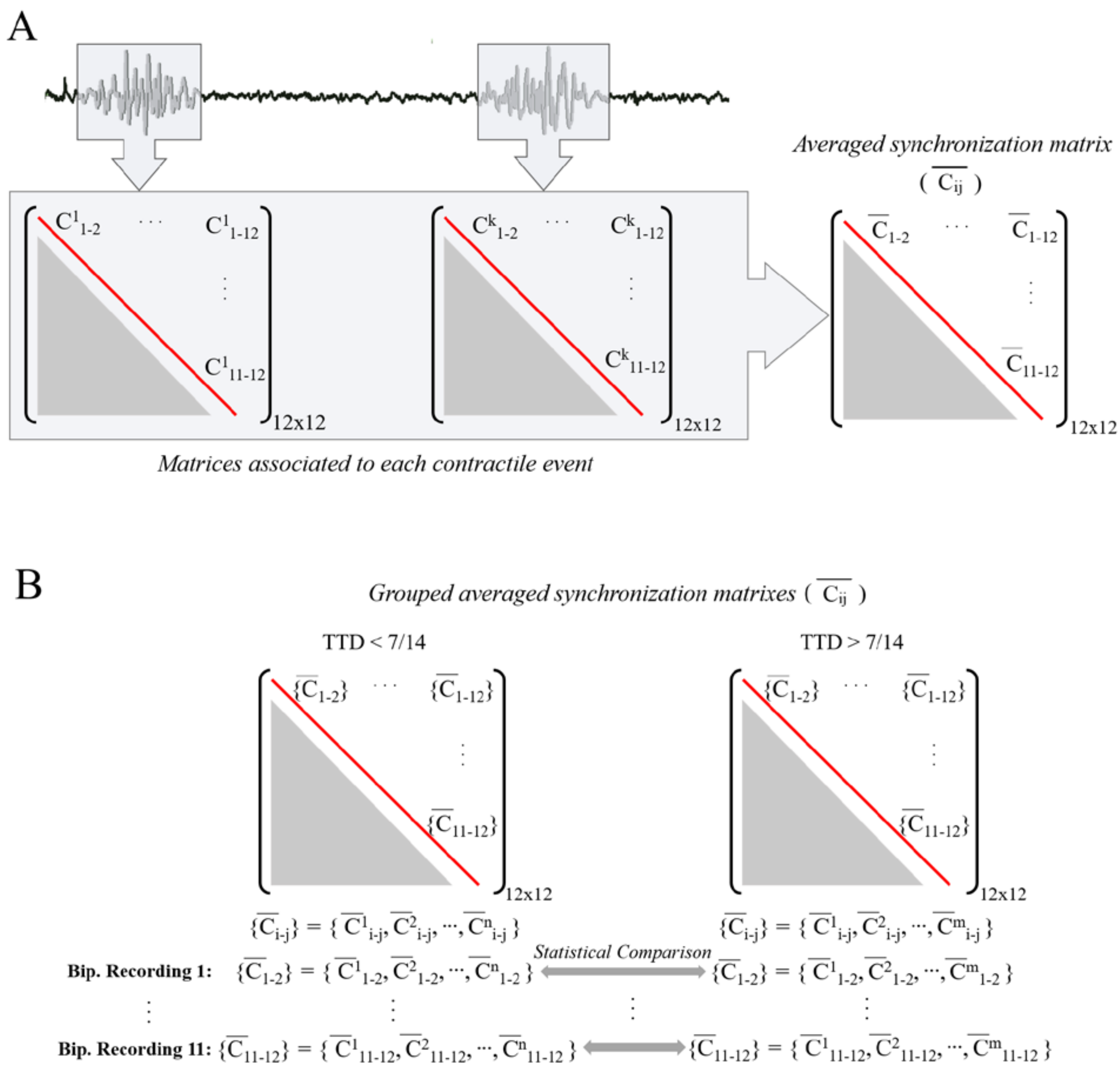

Figure 3: (A) Explanatory diagram of the average efficiency matrix ($\overline{C_{ij}}$) estimation method for each register, where C^k_{ij} is 12x12 efficiency matrix obtained from k^{th} uterine contractile event embedded in a recording session, sub-indexes i = 1…12 and j = 1…12 represent every bipolar record. (B) Statistical analysis of { $\overline{C_{ij}}$ } between groups according to TTD for each pair of bipolar recordings, where { $\overline{C_{ij}}$ } is the average efficiency index of all patients who belong to the same group and for a certain combination of bipolar records i and j, n is the number of patients who delivered in less than 7/14 and m represents the number of patients who delivered in more than 7/14 days.

3. RESULTS

Figure 4 shows 250 s of EHG signals recorded during pregnancy (left) and labor (right) from two different patients. Two uterine contraction events can be clearly appreciated in all the bipolar records in the labor register, and high amplitude EHG-bursts(≈ 260 μV) can be clearly identified in various bipolar signals (right image Figure 4). In contrast, in the pregnancy register (left image Figure 4), even though some EHG-bursts can be clearly seen in bipolar signals B9 and B12, in the other bipolar signals they have really small amplitude values (≈ 100 μV). The fact of clearly observing the same contractile events in a large number of channels for the labor recording means that uterine electrical activity is a more global and coordinated phenomenon during labor than during pregnancy, when it is seen as a poorly coordinated or local activity.

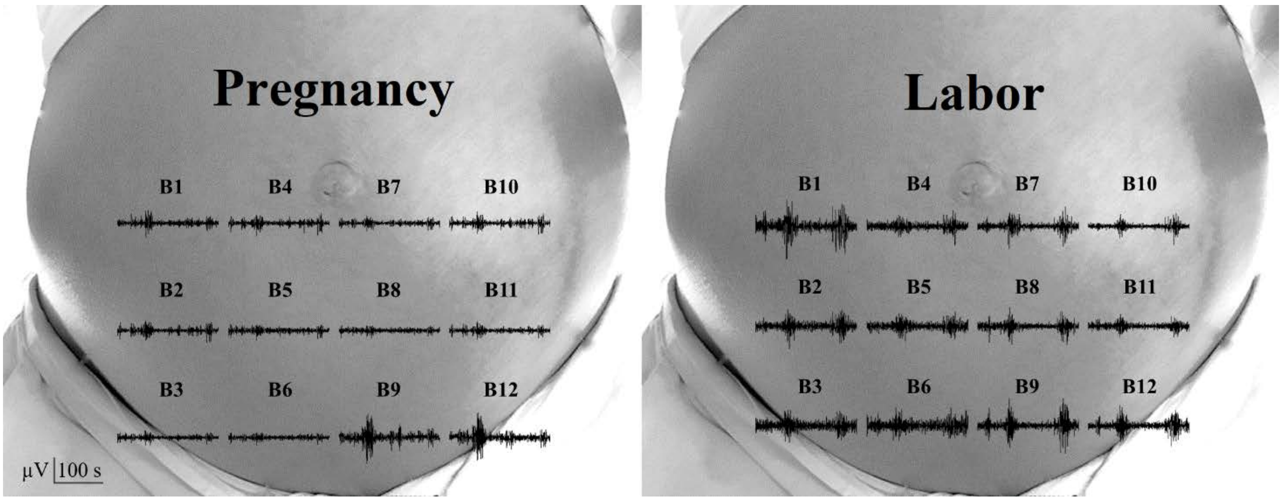

Figure 4: Twelve-channel preprocessed bipolar EHG registers of two different patients: (left) during pregnancy (22 days to labor); (right) during labor.

Figure 5 represents the different evolution of the MEI's efficiency indexes throughout pregnancy in the form of violin plots. It can be seen that both MEI_{MC_IEI} and MEI_{NPCMI}, show monotonic increasing trends as labor approaches. However, although MEI_{MC_EEI} and the other single-phenomenon efficiency indexes (MEI_{COR}, MEI_{iCOH} and MEI_{PLV}) tend to have higher values for the two groups close to labor, they show subtle increasing or even parabolic trends, while the MEIs of the four global efficiency indexes tend to increase as labor approaches and present similar monotonic increasing trends.

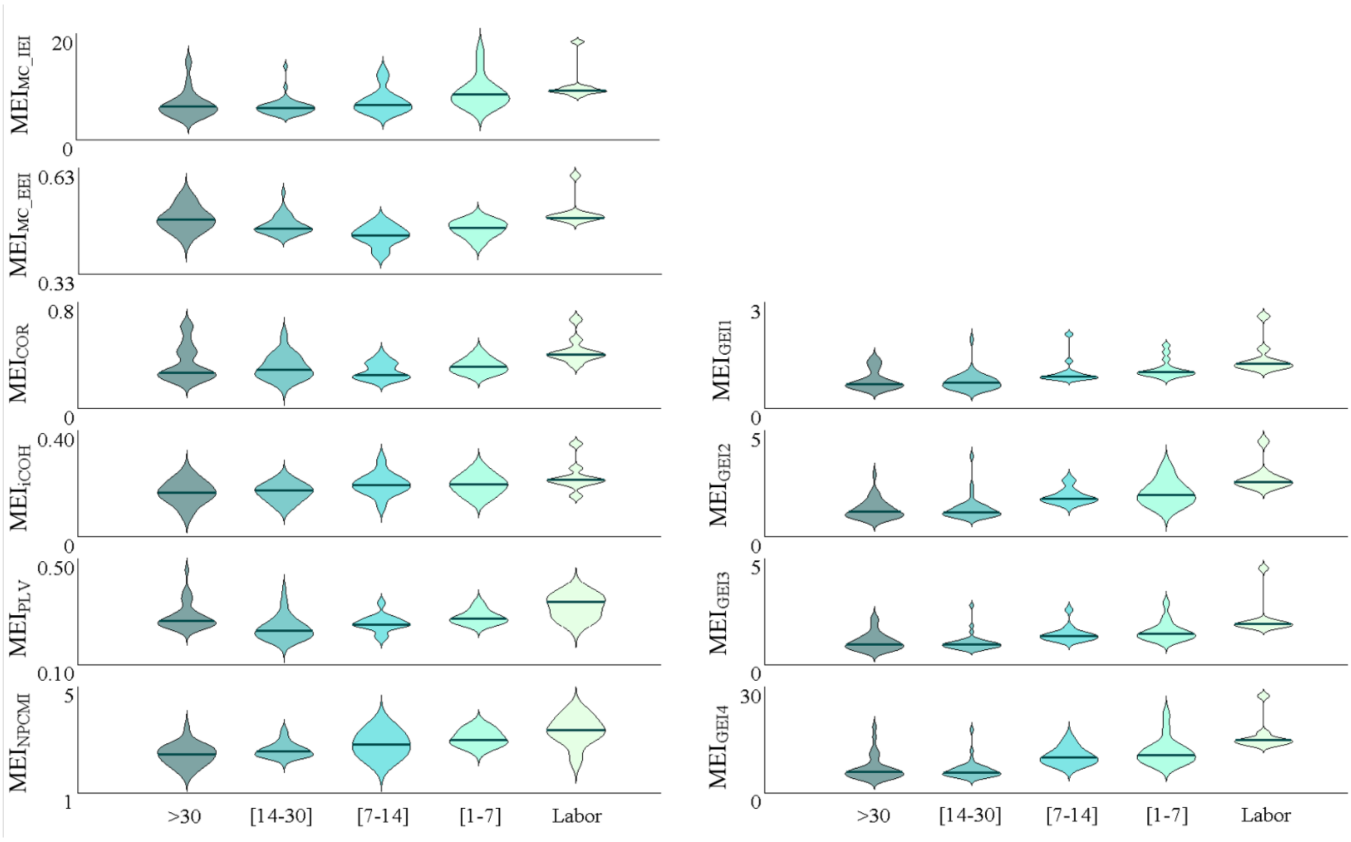

Figure 5: Violin plots of the different efficiency indexes' MEIs according to time-to-delivery. IEI: intensity efficiency indexes; EEI: excitability efficiency index; GEI1, GEI2, GEI3 and GEI4 are Global efficiency indexes using COR, iCOH, PLV and NPCMI as synchronization index (eq. 16-19).

The mean and standard deviation values of the different uterine MEIs are shown in Table 1. Most of the single-phenomenon MEIs (MEI_{MC_IEI}, MEI_{MC_EEI}, MEI_{COR}, MEI_{iCOH}, MEI_{PLV}, MEI_{NPCMI}) show higher values for women who delivered less than 7/14 days after the recording session than those who delivered after this time.

Single-phenomenon Efficiency Indexes				
TTD (days)	*<7*	*>7*	*<14*	*>14*
MEI_{MC_IEI} (μV)	6.67 ± 4.63	4.94 ± 3.23	6.35 ± 4.18	4.75 ± 3.19

MEI_{MC_EEI} (Hz)	0.453 ± 0.032	0.448 ± 0.03	0.450 ± 0.03	0.448 ± 0.031
MEI_{COR}	0.250 ± 0.091	0.234 ± 0.133	0.239 ± 0.102	0.235 ± 0.137
MEI_{iCOH}	0.197 ± 0.054	0.179 ± 0.048	0.193 ± 0.054	0.178 ± 0.046
MEI_{PLV}	0.328 ± 0.033	0.322 ± 0.046	0.325 ± 0.039	0.319 ± 0.046
MEI_{NPCMI}	2.85 ± 0.39	2.77 ± 0.36	2.85 ± 0.41	2.76 ± 0.35
	Global Efficiency Indexes			
TTD (days)	*<7*	*>7*	*<14*	*>14*
MEI_{GEI1} (μV·Hz)	0.751 ± 0.619	0.520 ± 0.438	0.678 ± 0.589	0.513 ± 0.418
MEI_{GEI2} (μV·Hz)	1.440 ± 0.992	0.976 ± 0.705	1.332 ± 0.858	0.938 ± 0.73
MEI_{GEI3} (μV·Hz)	1.066 ± 1.037	0.747 ± 0.533	0.962 ± 0.879	0.738 ± 0.541
MEI_{GEI4} (μV·Hz)	8.36 ± 5.728	5.89 ± 3.76	7.78 ± 4.89	5.70 ± 3.90

Table 1: Mean and standard deviation of the different uterine efficiency indexes for women who delivered in less than 7/14 days when using 4x4 matrix electrode.

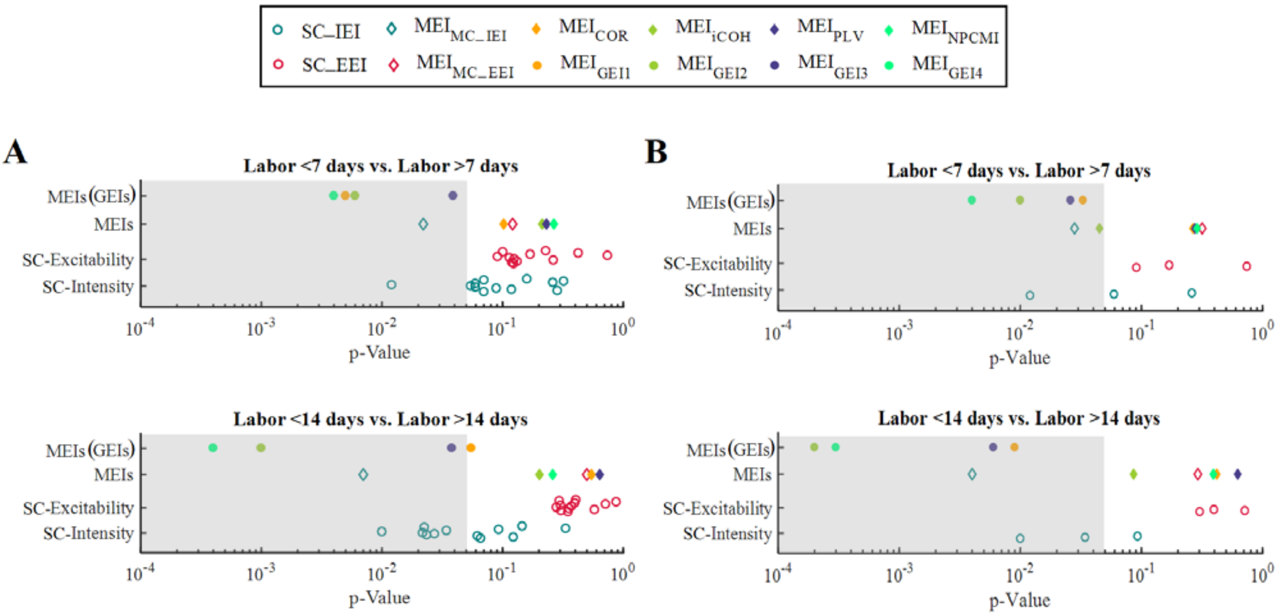

Figure 6: p-Value associated with separation of labor in less than 7/14 days of each type of parameter computed in the single channel and multichannel approaches, for the complete recording set (A) and for the reduced recording set (B).Grey area indicates p-value <0.05.

Figure 6 represents the p-values obtained to separate labor in less than 7/14 days for the efficiency indexes computed in a single channel (SC_IEI and SC_EEI) and multichannel approaches (MEI_{MC_IEI}, MEI_{MC_EEI}, MEI_{COR}, MEI_{iCOH}, MEI_{PLV}, MEI_{NPCMI}, MEI_{GEI1}, MEI_{GEI2}, MEI_{GEI3}, MEI_{GEI4}) for the complete recording set (frame A). For single-phenomenon parameters, only intensity parameters present significant differences ($p < 0.05$). Multichannel approach (MEI_{MC_IEI}) yielded lower p-values than single channel except for one case (B7, labor >7d vs.>7d).When IEI and the EEI are combined with synchronization indexes to bring out global efficiency indexes (MEI_{GEI1}, MEI_{GEI2}, MEI_{GEI3} and MEI_{GEI4}), the results show that all of them present statistically significant differences, except MEI_{GEI1} (labor <14d vs.>14d). Moreover, the p-values of global indexes are clearly lower than single-phenomenon for MEI_{GEI2} and MEI_{GEI4}. This latter shows the lowest p-values for detecting subjects who delivered in less than 7/14 days, which indicates better labor prediction for this efficiency index than the others.

The evolution of the GEI4 average efficiency matrix was also analyzed, i.e. the mean values of every bipolar recording combination for each group (labor, TTD<7d, TTD∈[7, 14[d, TTD∈[14,30[d, TTD>30d) according to time-to-delivery (see Figure 7). It can be clearly seen how GEI4 values tend to increase in all the elements of the matrix (bipolar recording combinations) for the TTD <7d group and reach their maximum values in the labor group.

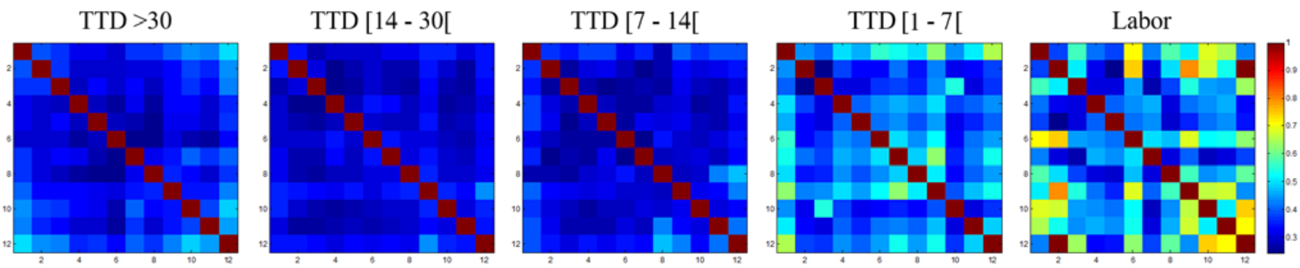

Figure 7: Evolution of mean GEI4 average efficiency matrix according to time-to-delivery.

Since GEI4 showed the most significant differences in detecting labor in less than 7/14 days it was chosen for inclusion in the simplified EHG data set. The number of elements (other bipolar recording channels) was computed of the GEI4 average efficiency matrix ($\overline{C_{ij}}$, j = 1…12 and $j \neq i$) that presented significant differences for differentiating subjects who delivered in less than 7/14 days (see Figure 8, where black dots represent electrodes, and rectangles the corresponding bipolar signals). Bipolar records B1, B4, B6, B7, B8, B9 and B11 show the largest number of significant differences with the other bipolar records. Bipolar signals B7, B8 and B9 (highlighted in dark blue in Figure 2) were selected for the simplified electrode configuration to discriminate between subjects liable to start labor in less or more than 7/14 days.

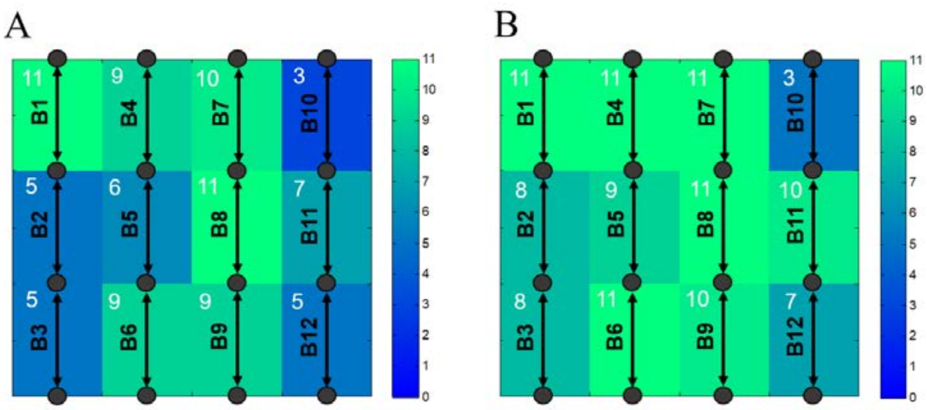

Figure 8: Representation of the number of elements with significant differences obtained by GEI4 in every bipolar record for the (A) TTD <7d vs TTD >7d and (B) TTD <14d vs TTD >14d comparisons.

Efficiency indexes were then worked out considering only this small number of bipolar records. The efficiency indexes' mean MEI values and standard deviations of the subjects who delivered in less than and more than 7/14 days are shown in Table 2. It can be seen that, as for the 4x4 electrode matrix, the MEIs tend to increase with higher values for labor in less than 7/14 days and lower values for labor in >7/14 days. Indeed, for the reduced recording set (only Channels B7-B8-B9) the p-values obtained were similar to those of the complete recording set (see Figure 6). Again, MEI$_{GEI2}$ and MEI$_{GEI4}$ indexes had the lowest p-value for separating subjects who delivered in less than 7/14 days.

Single-phenomenon Efficiency Indexes				
TTD (days)	*<7*	*>7*	*<14*	*>14*
MEI$_{MC_IEI}$(μV)	6.10 ± 3.81	4.931 ± 3.325	6.08 ± 3.71	4.66 ± 3.21
MEI$_{MC_EEI}$(Hz)	0.452 ± 0.036	0.443 ± 0.031	0.451 ± 0.034	0.447 ± 0.03
MEI$_{COR}$	0.241 ± 0.112	0.238 ± 0.154	0.234 ± 0.118	0.229 ± 0.159
MEI$_{iCOH}$	0.203 ± 0.066	0.178 ± 0.051	0.195 ± 0.061	0.177 ± 0.052
MEI$_{PLV}$	0.327 ± 0.042	0.321 ± 0.052	0.322 ± 0.045	0.323 ± 0.053
MEI$_{NPCMI}$	2.84 ± 0.41	2.746 ± 0.389	2.80 ± 0.425	2.736 ± 0.36

	Global Efficiency Indexes			
TTD (days)	*<7*	*>7*	*<14*	*>14*
MEI_{GEI1}	0.681 ± 0.527	0.520 ± 0.472	0.716 ± 0.61	0.463 ± 0.365
MEI_{GEI2}	1.342 ± 0.895	0.953 ± 0.645	1.332 ± 0.821	0.867 ± 0.603
MEI_{GEI3}	1.006 ± 0.949	0.759 ± 0.606	1.021 ± 0.953	0.679 ± 0.449
MEI_{GEI4}	7.53 ± 3.80	5.67 ± 3.66	7.29 ± 4.07	5.51 ± 3.75

Table 2: Mean and standard deviation of the different uterine efficiency indexes for women who delivered in less than 7/14 days when using the reduced electrode set (electrodes 9-12: B7, B8 and B9 records).

4. DISCUSSION

Labor prediction is of particular importance not only in women at risk of preterm labor but also in other obstetrical situations such as pharmacological labor induction, when accurate diagnosis could improve maternal-fetal wellbeing. A reliable system of predicting labor within 7 or even 14 days would permit the choice of the appropriate treatment, avoid unnecessary hospitalizations, and reduce healthcare costs. Accurate labor prediction is still one of the most challenging goals in obstetrics. Labor is associated with a change in the myometrial contractility pattern, which changes from "irregular contractions" (long lasting, low-frequency activity) to "regular contractions (high-intensity, high frequency activity, higher synchronization) [46]. However, the factors responsible for the onset of labor are still poorly understood, making the diagnosis of true labor difficult. It has been reported in the literature that EHG parameters provide better labor predictions than obstetrical indicators such as the Bishop Score or cervical length [10,47]. However, there are a number of barriers that must be overcome before EHG recordings can be used in clinical practice, for instance, the need for robust and easily interpretable EHG indexes. We thus propose a new global index based on the physiological phenomena (intensity, excitability and synchronization) of uterine activity which clinicians will find easy to interpret. This index has certain similarities in its conception with the Bishop Score, a parameter traditionally used in clinical practice, which combines information from different obstetrical features to obtain a single indicator of labor proximity [33]. On the other hand, these indexes combine information from different channels for robust estimations of the condition of the whole range of uterine myoelectrical activity.

As labor approaches, uterine contractions intensify so that EHG-burst amplitude increases and the signal spectral content is shifted to higher frequencies[48]. In our bivariate approach, this is reflected in an increase of the MC_IEI and MC_EEI, respectively. Since the computation of these indexes involves information embedded in pairs of bipolar records, they also inherently contain information on the degree of EHG coupling. The MEI_{MC_IEI} was found to show significant differences in the comparisons between TTD <7d vs. TTD >7d (*p*: 0.022) and TTD <14dvs. TTD >14d (*p*: 0.007). These results agree with previous findings of significant differences between the RMS amplitude values of patients who gave birth in more or less than 14 days [6]. However, although MEI_{MC_EEI} showed a slight increase as labor approaches, in line with previous studies [49,30], it does not seem to provide relevant information on predicting labor onset as reported by other authors who also performed a whole EHG register analysis [25]. Some studies reported that the spectral content shifts toward higher frequencies around 24h before labor, while others found a shift towards lower frequencies 10 days before delivery [50]. These results agree with the parabolic trend shown by the EEI in the present study.

It has also been shown that signal synchronization increases as labor approaches [16,18]. In the present work we studied the performance of different synchronization indexes (COR, iCOH, PLV and NPCMI) to assess the evolution of EHG-burst synchronization in late pregnancy. The single-phenomenon efficiency values tend to increase as labor approaches, showing that the uterine electrical activity becomes more intense and coordinated due to an increase of gap junctions between the myometrial cells [51]. Our COR, iCOH and PLV results agree with previous findings that also reported higher synchronization index values for higher degrees of coupling [18,44]. NPCMI, which provided promising results in EEG applications, has never been used to estimate the degree of synchronization of EHG signals. The results obtained by the NPCMI point in the same direction as the other above-mentioned synchronization indexes, suggesting stronger synchronization between multichannel EHG signals as labor approaches. According to the results obtained, the synchronization indexes by themselves do not seem able to predict the onset of labor in the 7/14-day intervals studied.

The GEIs, which combine estimators of signal intensity, cell excitability and signal synchronization, could be useful in distinguishing between different time-to-delivery horizons. To the authors' knowledge, there are no existing studies of EHG global efficiency indexes that take into account the three phenomena involved in uterine contractility. Again, the four GEIs were found to increase as labor approaches. It should be noted that these trends are monotonic, in contrast to those found in the single-phenomenon synchronization indexes, which may present parabolic trends (COR and PLV), which is not in accordance with the myoelectrical activity efficiency concept. Furthermore, when using a 4x4 matrix electrode, all the GEIs defined in this work, except GEI1, showed significant differences for distinguishing labor in less than 7/14 days and had lower p-values than single-phenomenon efficiency indexes computed in just one channel. This may suggest that myoelectrical activity efficiency is mainly due to signal amplitude, although the interaction with cell excitability and synchronization measurement could truly contain relevant complementary information on labor onset and provide promising results for predicting labor in less than 7/14 days.

Since the use of 16 electrodes for EHG signal recording may not be acceptable in a clinical setting, a simplified 3 bipolar channel-based analysis was proposed, for which signal quality was one of the criteria for the selection of this subset of channels. Previous studies have shown that signals with better signal-to-noise ratios are usually obtained from the records of electrodes located in the uterine midline (fundus to pubic symphysis) and in the mid-central axis of the uterus [27,40]. In the present work the horizontal line formed by bipolar records B1, B4 and B7 present almost the same number of cases with significant differences as the vertical line formed by B7, B8 and B9, although the latter was finally selected because it is aligned with the uterine median axis. In this location, the electrodes are closer to the uterus and the spectral content of the EHG has higher energy in the FWH, which would also provide higher discrimination [22]. Furthermore, only four electrodes are needed to obtain B7, B8 and B9 against the six required for B1, B4 and B7. The 3 channel subset associated with the simplified recording system proposed here has been shown to provide relevant information for labor prediction. When using only B7, B8 and B9, although not all the indexes improved their performance, the overall balance can be considered positive, since all the global efficiency indexes kept their discriminating ability. The multichannel efficiency indexes can identify subjects who will deliver in less than 14 days even better when combined with the simplified recording system, which indicates that channels with lower SNR could give slightly distorted information and do not improve the ability to separate the groups.

When efficiency indexes are computed on multiple channels the results are better than those obtained by the individual single-channel approach, in which synchronization information is lost. These indexes can be used to analyze the uterine state in other obstetrical situations. Indeed, we have computed these indexes in the (3-channel) TPEHG data base to discriminate term from preterm labor and found that the preliminary results agree with the results given here. MEI_{GEI4} shows the lowest p-values to discriminate both groups (term vs. preterm) when compared to single channel intensity and excitability indexes. The proposed global efficiency indexes and an adapted version of the proposed methodology could also be applied to other obstetrical scenarios, such as predicting successful labor induction [52,53].

On the other hand, even though significant differences were obtained by several efficiency indexes in predicting labor in less than 7/14 days, the small size of the database used could limit the extrapolation of the results to global populations. Bigger databases would also help to develop and test machine learning classificatory tools to further evaluate the discriminatory capacity of the proposed parameters.

Future work will involve more comprehensive databases to corroborate and provide greater generalization capacity. Non-linear parameters, such as sample entropy or time reversibility, which have shown positive results [25,54], will be considered. Furthermore, since labor is associated with more intense uterine dynamics and cervical ripening, the combination of EHG techniques (related to uterine contractile activity) and ultrasounds (for cervical length measurement) can be expected to give better preterm labor predictions. Besides cervical length, other traditional obstetric parameters, such as the Bishop score, length, maternal age, parity, etc. could also help to put EHG parameters into a subject-specific context and provide complementary information.

5. CONCLUSIONS

Although increased synchronization of myoelectrical activity was observed as labor approached, no significant differences were found in the associated single-phenomenon efficiency parameters for predicting labor, except in the case of the intensity efficiency index based on ARV. In contrast, the four proposed multichannel global efficiency indexes, which take into account information on the three key phenomena involved in myoelectrical activity efficiency (amplitude, spectral content and synchronization degree) showed a monotonic increasing trend with time-to-delivery and better ability to predict labor in less than 7/14 days than single channel and single phenomenon parameters. A reduced electrode set is also proposed, consisting of 4 electrodes aligned with the uterine median line between the fundus and pubic symphysis, which maintains the capacity to predict labor and also shows promise for being used in clinical practice.

ACKNOWLEDGMENTS

The authors are grateful to Zhenhu Liang, of the Yanshan University, who provided essential information for computing the PLV and NPCMI synchronization indexes. This work was supported by the Spanish Ministry of Economy and Competitiveness and the European Regional Development Fund (DPI2015-68397-R, MINECO/FEDER).

REFERENCES

[1] R.E. Garfield, W.L. Maner, Biophysical methods of prediction and prevention of preterm labor: uterine electromyography and cervical light-induced fluorescence – new obstetrical diagnostic techniques., in: Preterm Birth, 2006: pp. 131–144.

[2] S. Petrou, The economic consequences of preterm birth duringthe first 10 years of life, BJOG An Int. J. Obstet. Gynaecol. 112 (2005) 10–15. doi:10.1111/j.1471-0528.2005.00577.x.

[3] S. Beck, D. Wojdyla, L. Say, A. Pilar Bertran, M. Meraldi, J. Harris Requejo, C. Rubens, R. Menon, P. Van Look, The worldwide incidence of preterm birth: a systematic review of maternal mortality and morbidity, Bull. World Health Organ. 88 (2010) 31–38. doi:10.2471/BLT.08.062554.

[4] A.B. Boots, L. Sanchez-Ramos, D.M. Bowers, A.M. Kaunitz, J. Zamora, P. Schlattmann, The short-term prediction of preterm birth: A systematic review and diagnostic metaanalysis, Am. J. Obstet. Gynecol. 210 (2014) 54.e1-54.e10. doi:10.1016/j.ajog.2013.09.004.

[5] D.M. Haas, T. Benjamin, R. Sawyer, S.K. Quinney, Short-term tocolytics for preterm delivery - Current perspectives, Int. J. Womens. Health. 6 (2014) 343–349. doi:10.2147/IJWH.S44048.

[6] O. Most, O. Langer, R. Kerner, G. Ben David, I. Calderon, Can myometrial electrical activity identify patients in preterm labor?, Am. J. Obstet. Gynecol. 199 (2008) 378. doi:10.1016/j.ajog.2008.08.003.

[7] H. de Lau, C. Rabotti, H.P. Oosterbaan, M. Mischi, G.S. Oei, Study protocol: PoPE-Prediction of Preterm delivery by Electrohysterography, BMC Pregnancy Childbirth. 14 (2014) 192. doi:10.1186/1471-2393-14-192.

[8] R.E. Garfield, W.L. Maner, H. Maul, G.R. Saade, Use of uterine EMG and cervical LIF in monitoring pregnant patients., Int. J. Obstet. Gynaecol. 112 (2005) 103–108. doi:10.1111/j.1471-0528.2005.00596.x.

[9] K. Lim, K. Butt, J.M. Crane, No. 257-Ultrasonographic Cervical Length Assessment in Predicting Preterm Birth in Singleton Pregnancies, J. Obstet. Gynaecol. Canada. 40 (2018) e151–e164. doi:10.1016/j.jogc.2017.11.016.

[10] T.Y. Euliano, M.T. Nguyen, S. Darmanjian, S.P. McGorray, N. Euliano, A. Onkala, A.R. Gregg, Monitoring uterine activity during labor: A comparison of 3 methods, Am. J. Obstet. Gynecol. 208 (2013) 66.e1-66.e6. doi:10.1016/j.ajog.2012.10.873.

[11] E. Hadar, T. Biron-Shental, O. Gavish, O. Raban, Y. Yogev, A comparison between electrical uterine monitor, tocodynamometer and intra uterine pressure catheter for uterine activity in labor, J. Matern. Neonatal Med. 28 (2015) 1367–1374. doi:10.3109/14767058.2014.954539.

[12] R.E. Garfield, W.L. Maner, Physiology and electrical activity of uterine contractions, Semin. Cell Dev. Biol. 18 (2007) 289–295. doi:10.1016/j.semcdb.2007.05.004.

[13] J. Garcia-Casado, Y. Ye-Lin, G. Prats-Boluda, J. Mas-Cabo, J. Alberola-Rubio, A. Perales, Electrohysterography in the diagnosis of preterm birth: a review, Physiol. Meas. (2018). doi:10.1088/1361-6579/aaad56.

[14] P. Fergus, P. Cheung, A. Hussain, D. Al-Jumeily, C. Dobbins, S. Iram, Prediction of Preterm Deliveries from EHG Signals Using Machine Learning, PLoS One. 8 (2013). doi:10.1371/journal.pone.0077154.

[15] H. Maul, W.L. Maner, G. Olson, G.R. Saade, R.E. Garfield, Non-invasive transabdominal uterine electromyography correlates with the strength of intrauterine pressure and is predictive of labor and delivery., J. Matern. Neonatal Med. 15 (2004) 297–301.

doi:10.1080/14767050410001695301.

[16] M. Lucovnik, W.L. Maner, L.R. Chambliss, R. Blumrick, J. Balducci, Z. Novak-antolic, R.E. Garfield, Noninvasive uterine electromyography for prediction of preterm delivery, Am. J. Obstet. Gynecol. Gynecol. 204 (2011) 228.e1-228.e10. doi:10.1016/j.ajog.2010.09.024.

[17] D. Alamedine, A. Diab, C. Muszynski, B. Karlsson, M. Khalil, C. Marque, Selection algorithm for parameters to characterize uterine EHG signals for the detection of preterm labor, Signal, Image Video Process. 8 (2014) 1169–1178. doi:10.1007/s11760-014-0655-2.

[18] N. Nader, M. Hassan, W. Falou, A. Diab, S. Al-Omar, M. Khalil, C. Marque, Classification of pregnancy and labor contractions using a graph theory based analysis, in: Proc. Annu. Int. Conf. IEEE Eng. Med. Biol. Soc. EMBS, 2015: pp. 2876–2879. doi:10.1109/EMBC.2015.7318992.

[19] M. Hassan, J. Terrien, A. Alexandersson, C. Marque, B. Karlsson, Improving the classification rate of labor vs. normal pregnancy contractions by using EHG multichannel recordings, 2010 Annu. Int. Conf. IEEE Eng. Med. Biol. Soc. EMBC'10. (2010) 4642–4645. doi:10.1109/IEMBS.2010.5626486.

[20] Z. Liang, Y. Ren, J. Yan, D. Li, L.J. Voss, J.W. Sleigh, X. Li, A comparison of different synchronization measures in electroencephalogram during propofol anesthesia, J. Clin. Monit. Comput. 30 (2016) 451–466. doi:10.1007/s10877-015-9738-z.

[21] W.L. Maner, R.E. Garfield, Identification of human term and preterm labor using artificial neural networks on uterine electromyography data, Ann. Biomed. Eng. 35 (2007) 465–473. doi:10.1007/s10439-006-9248-8.

[22] C.K. Marque, J. Terrien, S. Rihana, G. Germain, E.C.K. Marque, J. Terrien, S.R. Sandyrihanautcfr, G. Germain, Preterm labour detection by use of a biophysical marker : the

uterine electrical activity, 7 (2007) 1–6. doi:10.1186/1471-2393-7-S1-S5.

[23] A. Smrdel, F. Jager, Separating sets of term and pre-term uterine EMG records, Physiol. Meas. 36 (2015) 341–355. doi:10.1088/0967-3334/36/2/341.

[24] A. Lemancewicz, M. Borowska, P. Kuć, E. Jasińska, P. Laudański, T. Laudański, E. Oczeretko, Early diagnosis of threatened premature labor by electrohysterographic recordings - The use of digital signal processing, Biocybern. Biomed. Eng. 36 (2016) 302–307. doi:10.1016/j.bbe.2015.11.005.

[25] G. Fele-Žorž, G. Kavšek, Ž.ˇNovak-Antolič, F. Jager, A comparison of various linear and non-linear signal processing techniques to separate uterine EMG records of term and pre-term delivery groups, Med. Biol. Eng. Comput. 46 (2008) 911–922. doi:10.1007/s11517-008-0350-y.

[26] A. Alexandersson, T. Steingrimsdottir, J. Terrien, C. Marque, B. Karlsson, The Icelandic 16-electrode electrohysterogram database, Sci. Data. 2 (2015) 150017. doi:10.1038/sdata.2015.17.

[27] J. Alberola-Rubio, J. Garcia-Casado, Y. Ye-Lin, G. Prats-Boluda, A. Perales, Recording of electrohysterogram laplacian potential, Proc. Annu. Int. Conf. IEEE Eng. Med. Biol. Soc. EMBS. (2011) 2510–2513. doi:10.1109/IEMBS.2011.6090695.

[28] J. Alberola-Rubio, G. Prats-Boluda, Y. Ye-Lin, J. Valero, A. Perales, J. Garcia-Casado, Comparison of non-invasive electrohysterographic recording techniques for monitoring uterine dynamics, Med. Eng. Phys. 35 (2013) 1736–1743. doi:10.1016/j.medengphy.2013.07.008.

[29] C. Rabotti, M. Mischi, J. Van Laar, G. Oei, J. Bergmans, Electrohysterographic analysis of uterine contraction propagation with labor progression: A preliminary study, Annu. Int. Conf.

IEEE Eng. Med. Biol. - Proc. (2007) 4135–4138. doi:10.1109/IEMBS.2007.4353246.

[30] D. Schlembach, W.L. Maner, R.E. Garfield, H. Maul, Monitoring the progress of pregnancy and labor using electromyography, Eur. J. Obstet. Gynecol. Reprod. Biol. 144 (2009) 2–8. doi:10.1016/j.ejogrb.2009.02.016.

[31] A. Chkeir, M.J. Fleury, B. Karlsson, M. Hassan, C. Marque, Patterns of electrical activity synchronization in the pregnant rat uterus, Biomed. 3 (2013) 140–144. doi:10.1016/j.biomed.2013.04.007.

[32] E. Hadar, N. Melamed, A. Aviram, O. Raban, L. Saltzer, L. Hiersch, Y. Yogev, Effect of an oxytocin receptor antagonist (atosiban) on uterine electrical activity, Am. J. Obstet. Gynecol. 209 (2013) 384.e1-384.e7. doi:10.1016/j.ajog.2013.05.053.

[33] L. M, M. WL, C. LR, Noninvasive Uterine Electromyography For Prediction of Preterm Delivery, Am J Obs. Gynecol. 204 (2012) 1–20. doi:10.1016/j.ajog.2010.09.024.Noninvasive.

[34] M.P.G.C. Vinken, C. Rabotti, M. Mischi, S.G. Oei, Accuracy of Frequency-Related Parameters of the Electrohysterogram for Predicting Preterm Delivery, Obstet. Gynecol. Surv. 64 (2009) 529–541. doi:10.1097/OGX.0b013e3181a8c6b1.

[35] K. Horoba, J. Jezewski, A. Matonia, J. Wrobel, R. Czabanski, M. Jezewski, Early predicting a risk of preterm labour by analysis of antepartum electrohysterograhic signals, Biocybern. Biomed. Eng. 36 (2016) 574–583. doi:10.1016/j.bbe.2016.06.004.

[36] P. Fergus, I. Idowu, A. Hussain, C. Dobbins, Advanced artificial neural network classification for detecting preterm births using EHG records, Neurocomputing. 188 (2016) 42–49. doi:10.1016/j.neucom.2015.01.107.

[37] U.R. Acharya, V.K. Sudarshan, S. Qing, Z. Tan, M. Lim, J. Ew, S. Nayak, S. V Bhandary, Automated detection of premature delivery using empirical mode and wavelet packet

decomposition techniques with uterine electromyogram signals, Comput. Biol. Med. 85 (2017) 33–42. doi:10.1016/j.compbiomed.2017.04.013.

[38] F.S. Ayachi, S. Boudaoud, C. Marque, Evaluation of muscle force classification using shape analysis of the sEMG probability density function: a simulation study, Med. Biol. Eng. Comput. 52 (2014) 673–684. doi:10.1007/s11517-014-1170-x.

[39] Y. Ye-Lin, J. Alberola-Rubio, G. Prats-boluda, A. Perales, D. Desantes, J. Garcia-Casado, Feasibility and Analysis of Bipolar Concentric Recording of Electrohysterogram with Flexible Active Electrode, Ann. Biomed. Eng. 43 (2015) 968–976. doi:10.1007/s10439-014-1130-5.

[40] J. Terrien, C. Marque, B. Karlsson, Spectral characterization of human EHG frequency components based on the extraction and reconstruction of the ridges in the scalogram, Annu. Int. Conf. IEEE Eng. Med. Biol. - Proc. (2007) 1872–1875. doi:10.1109/IEMBS.2007.4352680.

[41] G. Siegle, MATLAB Toolbox for Functional Connectivity Dongli, Neuroimage. 47 (2009) 1590–1607. doi:10.1016/j.neuroimage.2009.05.089.MATLAB.

[42] G. Nolte, O. Bai, L. Wheaton, Z. Mari, S. Vorbach, M. Hallett, Identifying true brain interaction from EEG data using the imaginary part of coherency, Clin. Neurophysiol. 115 (2004) 2292–2307. doi:10.1016/j.clinph.2004.04.029.

[43] D. Li, L.J. Voss, J.W. Sleigh, X. Li, D. Ph, Effects of volatile anesthetic agents on cerebral cortical synchronization in sheep., Anesthesiology. 119 (2013) 81–8. doi:10.1097/ALN.0b013e31828e894f.

[44] V. Sakkalis, C. Doru Giurcăneanu, P. Xanthopoulos, M.E. Zervakis, V. Tsiaras, Y. Yang, E. Karakonstantaki, S. Micheloyannis, Assessment of linear and nonlinear synchronization measures for analyzing EEG in a mild epileptic paradigm, in: IEEE Trans. Inf. Technol.

Biomed., 2009: pp. 433–441. doi:10.1109/TITB.2008.923141.

[45] D. Cui, W. Pu, J. Liu, Z. Bian, Q. Li, L. Wang, G. Gu, A new EEG synchronization strength analysis method: S-estimator based normalized weighted-permutation mutual information, Neural Networks. 82 (2016) 30–38. doi:10.1016/j.neunet.2016.06.004.

[46] J.B. Liao, C.S. Buhimschi, E.R. Norwitz, Normal labor: Mechanism and duration, Obstet. Gynecol. Clin. North Am. 32 (2005) 145–164. doi:10.1016/j.ogc.2005.01.001.

[47] R. Garfield, W. Maner, Biophysical methods of prediction and prevention of preterm labor, in: Preterm Birth, CRC Press, 2007: pp. 131–144. doi:doi:10.1201/b13792-16.

[48] C. Buhimschi, M.B. Boyle, G.R. Saade, R.E. Garfield, Uterine activity during pregnancy and labor assessed by simultaneous recordings from the myometrium and abdominal surface in the rat, Am. J. Obstet. Gynecol. 178 (1998) 811–822. doi:10.1016/S0002-9378(98)70498-3.

[49] D. Devedeux, C. Marque, S. Mansour, G. Germain, J. Duchêne, Uterine electromyography: A critical review, Am. J. Obstet. Gynecol. 169 (1993) 1636–1653. doi:10.1016/0002-9378(93)90456-S.

[50] W.L. Maner, R.E. Garfield, H. Maul, G. Olson, G. Saade, Predicting Term and Preterm Delivery With Transabdominal Uterine Electromyography, Obstet. Gynecol. 101 (2003) 1254–1260. doi:10.1016/S0029-7844(03)00341-7.

[51] R.E. Garfield, R.H. Hayashi, Appearance of gap junctions in the myometrium of women during labor, Am. J. Obstet. Gynecol. 140 (1981) 254–260. doi:10.5555/uri:pii:0002937881902702.

[52] R.L. Goldenberg, J.F. Culhane, J.D. Iams, R. Romero, Epidemiology and causes of preterm birth, Lancet. 371 (2008) 75–84. doi:10.1016/S0140-6736(08)60074-4.

[53] J. Vrhovec, A.M. Lebar, An Uterine Electromyographic Activity as a Measure of Labor

Progression, Appl. EMG Clin. Sport. Med. (2012) 243–268. doi:10.5772/25526.

[54] M. Hassan, J. Terrien, C. Marque, B. Karlsson, Comparison between approximate entropy, correntropy and time reversibility: Application to uterine electromyogram signals, Med. Eng. Phys. 33 (2011) 980–986. doi:10.1016/j.medengphy.2011.03.010.

List of Figures

Figure 1: Distribution of registers according to time-to-delivery (in days).

Figure 2: Electrode numbering scheme of the Icelandic data-base and method of calculating bipolar signals (adapted from the original work on "Icelandic 16-electrode database" [26]).

Figure 3: (A) Explanatory diagram of the average efficiency matrix ($\overline{C_{ij}}$) estimation method for each register, where C^k_{ij} is 12x12 efficiency matrix obtained from kth uterine contractile event embedded in a recording session, sub-indexes i = 1…12 and j = 1…12 represent every bipolar record. (B) Statistical analysis of { $\overline{C_{ij}}$ } between groups according to time-to-delivery for each pair of bipolar recordings (B), where { $\overline{C_{ij}}$ } is the average efficiency index of all patients who belong to the same group and for a certain combination of bipolar records i and j, n is the number of patients who delivered in less than 7/14 and m represents the number of patients who delivered in more than 7/14 days.

Figure 4: Twelve-channel preprocessed bipolar EHG registers of two different patients: (left) during pregnancy (22 days to labor); (right) during labor.

Figure 5: Violin plots of the different efficiency indexes' MEIs according to time-to-delivery. IEI: intensity efficiency indexes; EEI: excitability efficiency index; GEI1, GEI2, GEI3 and GEI4 are Global efficiency indexes using COR, iCOH, PLV and NPCMI as synchronization index (eq. 16-19).

Figure 6:p-Value associated with separation of labor in less than 7/14 days of each type of parameter computed in the single channel and multichannel approaches, for the complete recording set (A) and for the reduced recording set (B). Grey area indicates p-value <0.05.

Figure 7: Evolution of mean GEI4 average efficiency matrix according to time-to -delivery.

Figure 8: Representation of the number of elements with significant differences obtained by GEI4 in every bipolar record for the (A) TTD <7d vs TTD >7d and (B) TTD <14d vs TTD >14d comparisons.

List of Tables